DOI: 10.1002/zaac.201100355

Synthesis and Structural Diversity of $ZnCl_2$ and $Zn(C_6F_5)_2$ Complexes of a Phosphinimine Ligand

Craig A. Wheaton,[a] Benjamin J. Ireland,[a] and Paul G. Hayes*[a]

Keywords: Phosphinimine; Zinc; N,O ligands; X-ray diffraction; Dibenzofuran

Abstract. Zinc complexes of the potentially bidentate neutral monophosphinimine ligand 4-(ArN=PPh_2)dibenzofuran were prepared. Two derivatives of this framework were studied, which differ in the steric demand of the N-aryl group (Ar = Dipp, Mes). The ligand interacts with diethylzinc in solution but does not form a tightly bound complex, whereby the degree of association is found to be dependent on temperature. However, isolable complexes are formed upon reaction with the more Lewis acidic precursors $ZnCl_2$ and $Zn(C_6F_5)_2$. In this way, the $ZnCl_2$ complexes **1** and **2** and $Zn(C_6F_5)_2$ complexes **3** and **4** were prepared and structurally characterized. The nuclearity of **1** and **2** was shown to depend on the bulk of the ligand. Furthermore, the strength of the bonding interaction between the zinc atoms and the dibenzofuran oxygen atoms in **3** and **4** also depends on the choice of ancillary ligand. Attempts to further derivatize these complexes were unsuccessful, and thus, functionalization of the complex LZnEt(OTf) was undertaken instead, resulting in formation of the novel linear trinuclear complex **5**.

Introduction

Bidentate phosphinimine ligands, which have seen substantially increased use in recent years, were utilized to support a wide range of metals,[1] including early[2] and late transition metals,[3] rare-earth metals,[4] main group elements,[5] and a variety of zinc complexes.[6] The diverse applications found for these species include olefin polymerization,[2a] ring-opening polymerization of lactones,[4a,4b,6e] and hydroamination.[4d] We have been studying chemically robust, formally neutral phosphinimine ligand architectures for stabilizing cationic divalent metal atoms.[7] Our motivation for this work was to study the efficacy of such highly electrophilic complexes toward the ring-opening polymerization of lactones. However, the fundamental coordination chemistry of these scaffolds has remained largely unexplored. The presented report details the synthesis and characterization of several neutral zinc complexes of a monophosphinimine ligand, constructed by installation of a phosphinimine functionality at the 4-position of a rigid dibenzofuran (dbf) core. The insight gleaned from these studies regarding the fundamental properties of this hemilabile, potentially bidentate ligand framework, is described herein.

Results and Discussion

Ligand Synthesis and Characterization

The neutral ligands employed in this study were synthesized in one simple step from 4-diphenylphosphino-dibenzofuran by reaction with an appropriate aryl azide under standard Staudinger conditions.[8] Two derivatives of this architecture have been utilized, where the choice of N-aryl group was either 2,4,6-trimethylphenyl (Mes), $\mathbf{L^{Mes}}$, or 2,6-di*iso*propylphenyl (Dipp), $\mathbf{L^{Dipp}}$, which vary significantly in steric bulk. The preparation of $\mathbf{L^{Dipp}}$ was reported in a previous study,[7e] but this is the first account of the smaller analogue $\mathbf{L^{Mes}}$ (Scheme 1).

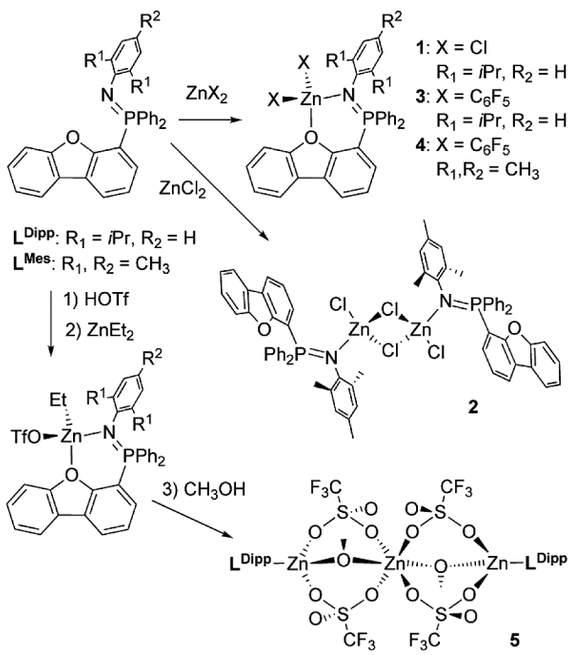

Scheme 1. Preparation of complexes **1**–**5**.

* Prof. Dr. P. Hayes
Fax: +01-403-329-2057
E-Mail: p.hayes@uleth.ca
[a] Department of Chemistry and Biochemistry
University of Lethbridge
E866 University Hall, 4401 University Drive
Lethbridge, Alberta, Canada

As discussed above, $\mathbf{L^{Mes}}$ was easily prepared by reaction of the precursor phosphine with mesityl azide. This afforded the ligand in 69% yield as an analytically pure powder that is indefinitely stable at ambient temperature when stored in an inert atmosphere. The diagnostic $^{31}P\{^1H\}$ NMR resonance appears at $\delta = -15.3$, which is upfield of the corresponding $\mathbf{L^{Dipp}}$ resonance by approximately 2 ppm.[7e] While the aromatic region of the ^1H NMR spectrum is complicated, the mesityl groups provide excellent spectroscopic handles, with singlet signals appearing at $\delta = 2.30$ and 2.21 ppm for the *para*- and *ortho*-CH_3 groups, respectively. Similarly, the *iso*propyl groups of $\mathbf{L^{Dipp}}$ provide diagnostic resonances in the aliphatic region of the ^1H spectrum. Single crystals of $\mathbf{L^{Mes}}$ were obtained and the crystal structure was determined (Figure 1), which serves to verify the connectivity of the molecule. The P–N bond length is in the expected range for a formal bond order of two [P(1)–N(1) = 1.547(3) Å], and is similar to that measured in the previously reported crystal structure of $\mathbf{L^{Dipp}}$ [1.559(2) Å],[7e] as well as other neutral phosphinimines.[9]

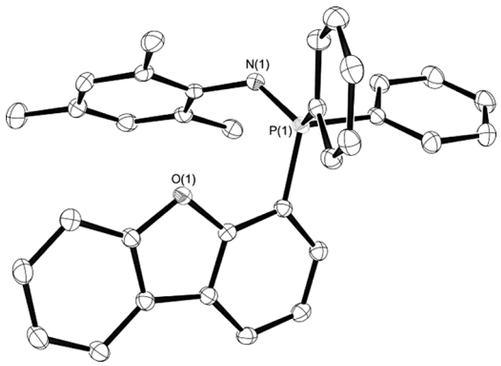

Figure 1. Thermal ellipsoid plot of one of two crystallographically unique molecules of $\mathbf{L^{Mes}}$ in the crystal lattice, with hydrogen-atoms and a molecule of toluene omitted for clarity. Thermal ellipsoids are drawn at the 30% probability level.

Reactivity with Diethylzinc

Our initial motivation for preparing these ligands was to eventually utilize them for the preparation of cationic heteroleptic zinc complexes. To that end, it was our desire to first prepare the neutral complex of diethylzinc, which would be converted into the cationic ethylzinc complex via alkide abstraction with a Lewis or Brønsted acid. However, reaction of $\mathbf{L^{Dipp}}$ with diethylzinc did not afford the anticipated result, but rather, it was discovered that exposure of the ligand to a single equiv. of diethylzinc resulted in little change in the spectroscopic features of the ligand. Specifically, the $^{31}P\{^1H\}$ NMR resonance was observed at $\delta = 12.6$ in [D_6]benzene, which only represented a 0.8 ppm downfield shift compared to the free ligand. This small change does not suggest a tightly bound complex, as the $^{31}P\{^1H\}$ NMR shift of phosphinimine moeities is well established to be much more sensitive to the presence of a metal atom. For example, a recent report by *Mehrkhodavandi* et al. examined a phosphinimine-imine ligand, which resonated at $\delta = 0.9$, and upon complexation of $ZnCl_2$ the resonance shifted to $\delta = 29.9$ ppm.[6b] Unsurprisingly, attempts to isolate a metal complex resulted in loss of diethylzinc upon removal of the solvent in vacuo, giving only the free ligand.

Exposure of $\mathbf{L^{Mes}}$ to diethylzinc in C_6D_6 caused a more perceptible change, resulting in a $^{31}P\{^1H\}$ NMR resonance at $\delta =$ 8.7 when three equiv. of diethylzinc were used. This represents a 6.6 ppm downfield shift relative to the free ligand. However, this change is still much smaller than expected for a tightly bound complex, and attempts to isolate this species again resulted only in liberation of the free ligand. Furthermore, despite the fact that three equiv. of the zinc reagent were employed, only one unique set of resonances attributed to the ethyl groups was observed in the ^1H NMR spectrum ($\delta = 1.19$ and 0.14 ppm for the CH_3 and CH_2 groups, respectively). This suggests an exchange process that is rapid on the NMR timescale due to labile metal-ligand bonding. Variable temperature NMR studies ([D_8]toluene) were performed in an attempt to garner more information about this equilibrium (Figure 2). It was found that the chemical shift of the ^{31}P signal is highly dependent on temperature, with more downfield shifts observed at lower temperatures (Figure 2). At –80 °C, the resonance appears at $\delta = 11.2$, which is 26.5 ppm downfield of the free ligand. These observations corroborate the idea that the system exists in equilibrium between the desired metal complex and the free starting materials. The fact that free $ZnEt_2$ and $\mathbf{L^{Mes}}$ are greatly favored at ambient temperature suggests a very weak metal-ligand interaction. Similar lability was noted for a related diazadiene ligand system.[10]

$ZnCl_2$ Complexes

Due to the inability to access neutral dialkylzinc complexes, we opted to pursue the preparation of species from much more electron deficient zinc precursors. All reactions were performed in non-coordinating solvents to prevent formation of solvent adducts, which could interfere with coordination of the weakly-binding ligand. Reaction of $\mathbf{L^{Dipp}}$ with $ZnCl_2$ required harsh conditions due to the poor solubility of the metal salt, but at 120 °C in toluene slow and irreversible conversion to a new species was observed. After 48 h, the reaction was complete and compound **1** was isolated as an analytically pure white powder in 65% yield. The complex exhibits a single signal in the $^{31}P\{^1H\}$ NMR spectrum at $\delta = 30.5$ ppm

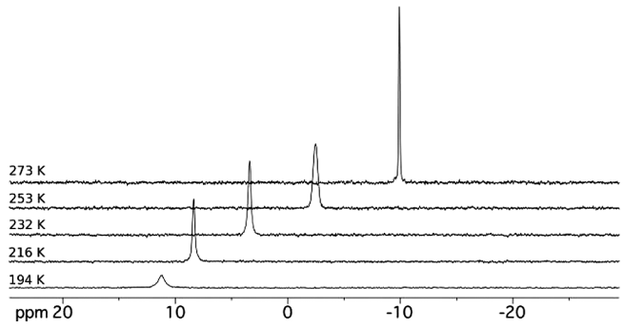

Figure 2. Variable temperature $^{31}P\{^1H\}$ NMR spectra of a C_6D_6 solution containing stoichiometric quantities of $\mathbf{L^{Mes}}$ and $ZnEt_2$.

Zeitschrift für anorganische und allgemeine Chemie ZAAC Journal of Inorganic and General Chemistry

(CD_2Cl_2), which is indicative of tight ligand coordination. Additionally, it was observed in the ^1H NMR spectrum that the *iso*propyl methyl groups were now inequivalent, giving rise to doublets at δ = 1.21 and 0.23 ppm. The complex is only sparingly soluble in aromatic solvents, and as a result some of the product crystallized on the walls of the reaction vessel during the course of the reaction. From this material, high quality single crystals were obtained, and the molecular structure of complex **1** was determined (Figure 3, Table 1).

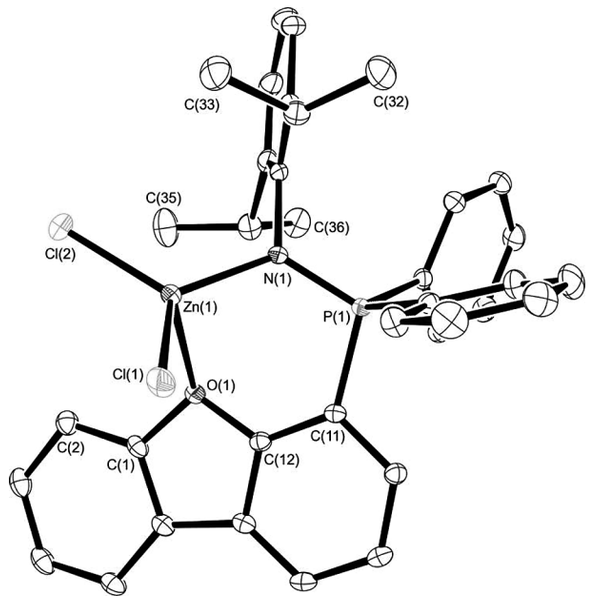

Figure 3. Thermal ellipsoid plot of complex **1**, with hydrogen atoms omitted for clarity. Thermal ellipsoids are drawn at the 30 % probability level.

Table 1. Selected bond lengths /Å and angles /° for the crystal structures of complexes **1** and **2**.

	1	**2**
Zn(1)–N(1)	1.960(1)	1.994(2)
Zn(1)–O(1)	2.381(1)	–
Zn(1)–Cl(1)	2.2003(3)	2.2048(8)
Zn(1)–Cl(2)	2.1713(4)	2.3437(9), 2.3450(9)
P(1)–N(1)	1.609(1)	1.609(2)
N(1)–Zn(1)–Cl(1)	120.87(3)	115.86(7)
N(1)–Zn(1)–Cl(2)	118.95(3)	107.47(7), 115.41(7)
Cl(1)–Zn(1)–Cl(2)	116.81(2)	112.18(4), 112.42(4)
Cl(1)–Zn(1)–O(1)	98.59(3)	–
P(1)–N(1)–Zn(1)	125.05(6)	124.4(1)
Zn(1)–Cl(2)–Zn(1b)	–	89.37(3)

The solid-state structure revealed that **1** is a monomeric complex, with the ligand bound to the zinc atom in a bidentate manner. The bond length between the phosphinimine nitrogen and the zinc atom is in the expected range [Zn(1)–N(1) = 1.960(1) Å], whereas the zinc oxygen contact is notably longer [Zn(1)–O(1) = 2.381(1) Å], suggesting a much weaker interaction. Furthermore, examination of the bond angles leads to the conclusion that the coordination is best described as distorted trigonal pyramidal. N(1), Cl(1), and Cl(2) occupy the equatorial sites with bond angles close to 120°; the sum of the angles about zinc is 356.63(5)°. Interestingly, the zinc atom sits significantly out of the plane defined by the dibenzofuran backbone (approx. 1.67 Å).

Complex **2** was prepared using $\mathbf{L^{Mes}}$ under similar reaction conditions as for **1**, giving an analytically pure white powder in approximately 89 % yield. This complex is dramatically less soluble than **1** in common organic solvents and correspondingly only ^1H and $^{31}P\{^1H\}$ NMR spectra were obtained. A single resonance was noted in the $^{31}P\{^1H\}$ NMR spectrum at δ = 28.0 ppm, while diagnostic mesityl peaks appear at δ = 2.01 (*o*-CH_3) and δ = 1.87 ppm (*p*-CH_3). Elemental analysis indicated the same stoichiometry of one ligand per $ZnCl_2$ unit; however, the limited solubility was suggestive of some degree of aggregation.

From material that had precipitated during the course of the reaction, a suitable single crystal of complex **2** was obtained and its solid-state structure was determined (Figure 4, Table 1). The structure confirms that aggregation does indeed occur, with the complex existing as a dimer in the solid state. The ligand does not adopt an orientation suitable for bidentate coordination, and thus, no interaction was noted between the zinc atom and the oxygen atom. Instead, the available coordination site is occupied by a bridging chloride Cl(2), giving rise to the observed dimeric structure. The two bridging chlorides are virtually equidistant between the zinc atoms with bond lengths of approximately 2.34 Å and a Zn(1)–Cl(2)–Zn(1b) angle approaching 90°. At 2.20 Å the terminal Zn–Cl distance is sub-

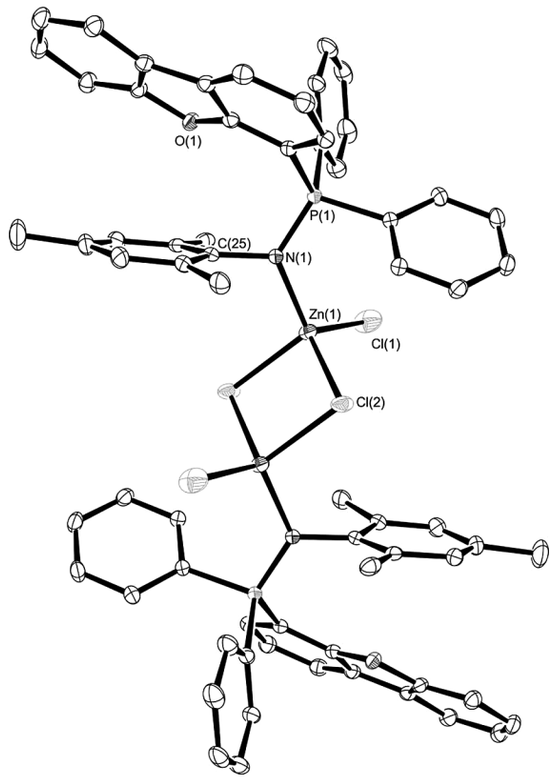

Figure 4. Thermal ellipsoid plot of the dimeric complex **2**, with hydrogen atoms and a disordered molecule of toluene omitted for clarity. Thermal ellipsoids are drawn at the 30 % probability level.

stantially shorter and the Zn–N length is within the normal range [1.994(2) Å]. In this case, the arrangement at zinc is most accurately described as four-coordinate tetrahedral.

The electronic properties of the ligands in **1** and **2** are highly similar; thus, it is reasonable to suggest that the large structural differences observed in the solid state are predominantly due to steric effects. In the less crowded **2**, dimerization is favored over the weak Zn–O interaction, whereas in complex **1**, the bulky *iso*propyl groups appear to prohibit this dimerization, forcing the zinc atom to interact with the dbf oxygen instead.

Zn(C$_6$F$_5$)$_2$ Complexes

Complexes of $Zn(C_6F_5)_2$ were more straightforward to prepare due to the higher solubility of the zinc precursor compared with $ZnCl_2$; complexation occurred immediately upon mixing the reagents in toluene solution. Reaction of $\mathbf{L^{Dipp}}$ with $Zn(C_6F_5)_2$ gave pale yellow crystals of complex **3** in 81% yield, while the corresponding reaction of $\mathbf{L^{Mes}}$ afforded **4** in 88% yield. Each complex exhibits a single resonance in the $^{31}P\{^1H\}$ NMR spectrum, with chemical shifts approximately 2 ppm upfield of the analogous $ZnCl_2$ complexes (**3**: δ = 28.5; **4**: δ = 25.7 ppm). The ^1H NMR spectra are also very similar to those observed for complexes **1** and **2**. For complex **3**, the *iso*propyl methyl resonances appear at δ = 1.11 and 0.38 ppm. In complex **4**, the *p*-CH_3 signal is again shifted upfield of the free ligand, to δ = 1.87 ppm. Both complexes exhibit high solubility in aromatic solvents, suggesting no significant aggregation. Single crystals of both **3** and **4** were grown from toluene/pentane solutions at –35 °C. The molecular structures are depicted in Figure 5 and Figure 6 for **3** and **4**, respectively, and selected metrical parameters for both complexes are located in Table 2.

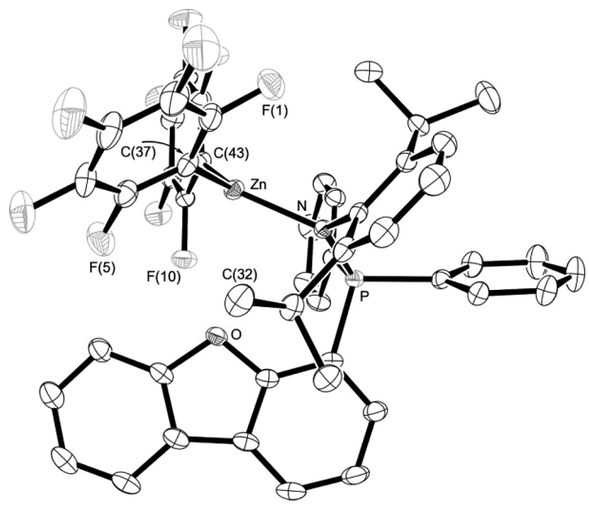

Figure 5. Thermal ellipsoid plot of complex **3**, with hydrogen atoms and solvent molecules omitted for clarity. Thermal ellipsoids are drawn at the 30% probability level.

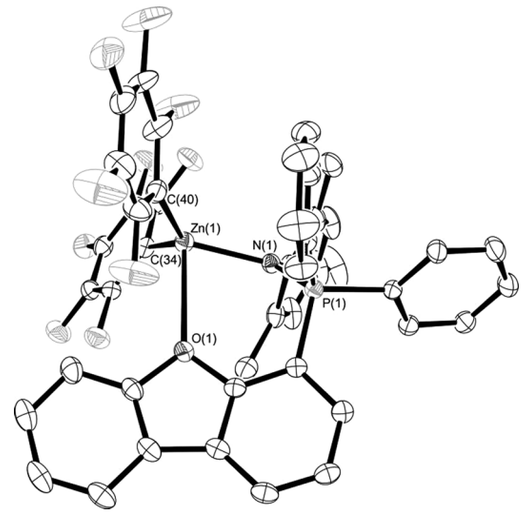

Figure 6. Thermal ellipsoid plot of complex **4**, with hydrogen atoms and a molecule of pentane omitted for clarity. Thermal ellipsoids are drawn at the 30% probability level.

Table 2. Selected bond lengths /Å and angles /° in complexes **3** and **4**.

	3	**4**
Zn–N	2.016(2)	2.006(2)
Zn–O	3.144(2)	2.669(2)
Zn–C(*x*)[a]	2.014(2)	2.014(2)
Zn–C(*y*)[a]	2.012(2)	2.010(3)
P–N	1.614(2)	1.603(2)
P–N–Zn	125.6(1)	122.1(1)
N–Zn–C(*x*)[a]	113.22(8)	108.33(9)
N–Zn–C(*y*)[a]	123.53(8)	119.94(9)
C(*x*)–Zn–C(*y*)[a]	122.18(9)	127.5(1)
N–Zn–O	74.39(6)	81.08(7)

a) **3**: *x* = 37, *y* = 43; **4**: *x* = 34, *y* = 40.

The solid state crystal structure of complex **3** corroborated its monomeric nature and revealed monodentate nitrogen coordination of the ligand. There is no meaningful bonding interaction between zinc and the dbf oxygen [Zn(1)–O(1) = 3.144(2) Å]. This bond is likely prevented from forming due to the sterically demanding C_6F_5 groups. The coordination arrangement is thus three-coordinate trigonal planar, rendering the zinc atom coordinatively unsaturated. The phosphinimine–Zn bond length lies within the usual range, as do the Zn–C bonds. The bond angles about these sites do not deviate significantly from 120°, with their sum totalling 358.9(1)°.

Complex **4** is essentially isostructural with **3**, with one notable exception being a significant Zn–O interaction [2.669(2) Å]. This is likely due to the sterically less demanding ancillary ligand, which permits a more suitable orientation for bidentate coordination. However, the steric requirements of the system remain high, thereby preventing a close contact (i.e. a typical Zn–O bond length of 2.0 Å). The sum of angles about zinc is reduced to 355.8(2)°, whereas the zinc atom lies 0.24 Å out of the plane defined by the coordinated nitrogen and carbon atoms (cf. 0.12 Å in **4** and 0.22 Å in **1**).

Zeitschrift für anorganische und allgemeine Chemie ZAAC Journal of Inorganic and General Chemistry

Other Complexes

Due to our interest in lactide polymerization catalysis, it was desirable to prepare a zinc alkoxide or amide species because such compounds are known to be excellent initiators for this transformation.[11] However, attempts to functionalize complexes **1**–**4** have met with little success. In particular, attempted salt metathesis reactions of the $ZnCl_2$ complexes with alkali metal amide or alkoxide salts appear to initially give the desired product. However, upon installation of amide or alkoxide functionalities, aggregation occurs resulting in release of the free ligand. While the C_6F_5 substituents of complexes **3** and **4** are not particularly amenable to derivatization, attempts were made to remove a C_6F_5 group using the protic salt $[HNMe_2][B(C_6F_5)_4]$. It was found, however, that upon reaction of **3** with this reagent, the acidic proton was simply transferred to the phosphinimine nitrogen with displacement of $Zn(C_6F_5)_2$, resulting in formation of the previously reported compound $[\mathbf{L^{Dipp}}H][B(C_6F_5)_4]$.[7e] Reaction of complex **4** with this same reagent produced a similar result.

Due to the inability to functionalize complexes **1**–**4**, we have instead explored derivatization of the previously reported alkylzinc compound $\mathbf{L^{Dipp}}$ZnEt(OTf).[7e,11b] It was anticipated that selective removal of the ethyl group by alkane elimination might be possible. In such a scenario, the weakly coordinating triflate group would be expected to maintain sufficiently high Lewis acidity at the metal atom to prevent ligand dissociation. Thus, $\mathbf{L^{Dipp}}$ZnEt(OTf) reacted with one equiv. of dry methanol in C_6D_6 and the reaction mixture was monitored by in situ NMR spectroscopy. Upon heating the solution to 100 °C for 1 h, ethane was observed at δ = 0.80 ppm in the ^{1}H NMR spectrum. The reaction mixture contained the free ligand and a new species which exhibited a broad ^{31}P NMR resonance at δ = 31.7 ppm, in approximately a 1:1 ratio. Within one day at ambient temperature, a significant amount of material had crystallized from the reaction mixture. This material proved too insoluble to characterize spectroscopically, but single crystals suitable for X-ray diffraction had formed, and so the solid-state structure was determined, revealing it to be the linear trinuclear zinc complex **5**. In order to give a balanced equation, complex **5** must arise with concomitant formation of 0.25 equiv. of dimethoxy zinc and 0.5 equiv. of free ligand (Scheme 2), which accounts for observation of free $\mathbf{L^{Dipp}}$ in the reaction mixture.

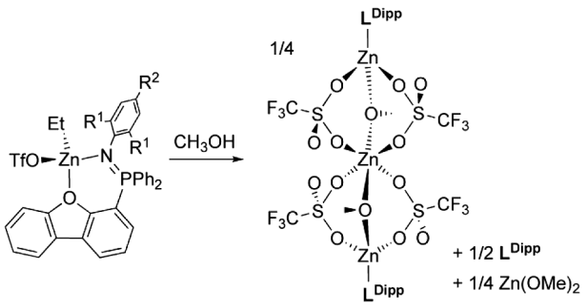

Scheme 2. Generation of complex **5** by reaction of $\mathbf{L^{Dipp}}$ZnEt(OTf) with one equiv. of methanol.

The molecular structure of complex **5** is depicted in Figure 7, and selected bond lengths and angles are given in Table 3. Two unique zinc atoms are present in the complex, with the central zinc [Zn(1)] occupying an inversion center. Each ligand is bound only through the phosphinimine nitrogen atom to a four-coordinate, tetrahedral zinc atom [Zn(2)], of which there are two in the complex. Both of these zinc atoms are also bound to two bridging triflate units and a bridging methoxide group, which connect to the central octahedral zinc atom [Zn(1)]. This complex can be considered as two molecules of the targeted complex linked by a $Zn(OTf)_2$ moiety. While it was surprising that this linear trinuclear zinc complex was formed, the structural motif is known in zinc chemistry and was first reported by *Clegg* and co-workers in 1985.[12] There are many examples reported since, although they typically incorporate acetate bridges.[13] Complex **5** is, to the best of our knowledge, the first example of a linear trinuclear zinc complex to incorporate either triflate or simple alkoxide bridges. Although formation of this complex was not the desired result, it does suggest potential for derivatization of neutral alkylzinc complexes of this type in the future.

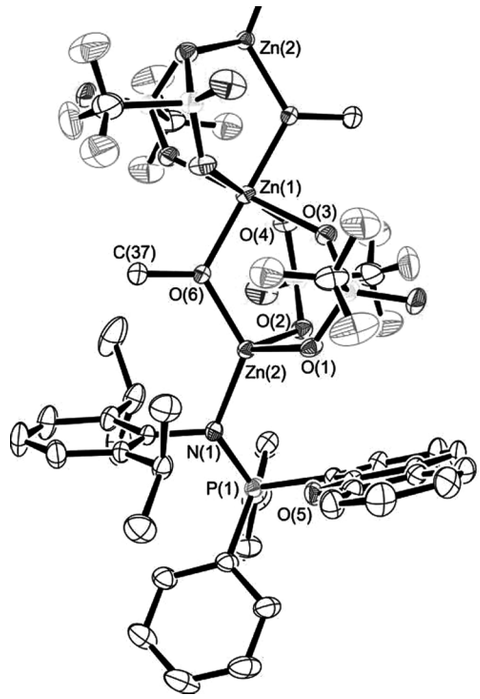

Figure 7. Thermal ellipsoid plot of complex **5**, with hydrogen atoms and a symmetry equivalent ligand omitted for clarity. Thermal ellipsoids are drawn at the 30% probability level.

Conclusions

It has been established that neither $\mathbf{L^{Dipp}}$ nor $\mathbf{L^{Mes}}$ bind strongly to diethylzinc, resulting instead in a solution equilibrium favoring the free ligand at ambient temperature. However, when more Lewis acidic zinc precursors were employed [$ZnCl_2$, $Zn(C_6F_5)_2$, and EtZnOTf], binding of the ligand was

Table 3. Selected bond lengths /Å and angles /° in the structure of **5**.

Atoms	Distances	Atoms	Angles
P(1)–N(1)	1.618(3)	N(1)–Zn(2)–O(1)	114.1(1)
Zn(2)–N(1)	1.944(2)	O(1)–Zn(2)–O(6)	104.21(9)
Zn(2)–O(1)	2.015(2)	N(1)–Zn(2)–O(2)	106.4(1)
Zn(2)–O(2)	2.023(2)	O(2)–Zn(2)–O(6)	101.65(9)
Zn(2)–O(6)	1.902(2)	Zn(2)–O(6)–Zn(1)	120.0(1)
Zn(1)–O(3)	2.200(2)	O(6)–Zn(1)–O(4)	90.77(8)
Zn(1)–O(4)	2.212(2)	O(6)–Zn(1)–O(3)	90.14(8)
Zn(1)–O(6)	1.968(2)	O(6)–Zn(1)–O(6_b)	180.00(8)

stronger and essentially irreversible. Crystallographic studies demonstrated that the binding mode of the ligand is either η^1 or κ^2, depending on the steric bulk of the N-aryl group of the ligand. In the case of $ZnCl_2$, the bulkier ligand prevents dimerization through bridging chloride groups, thereby promoting a weak Zn–O interaction. Conversely, in the case of $Zn(C_6F_5)_2$ complexes, the Zn–O interaction is inhibited by the bulkier perfluoroaryl moiety. Further functionalization of complexes **1**–**4** was unsuccessful; however, attempts to derivatize $\mathbf{L^{Dipp}}$ZnEt(OTf) by reaction with methanol afforded a novel linear trinuclear complex with unusual methoxy and triflate bridges. Overall, we have observed that variation in metal precursor and ligand substitution leads to an intriguing diversity of solution – and solid-state structures, which we hope to exploit in future studies.

Experimental Section

General: All manipulations of air-sensitive materials and reagents were conducted using high-vacuum techniques in a purified argon atmosphere or in a glove box (MBraun Labmaster 130). Protio solvents were purified with an MBraun solvent purification system (MB-SPS), stored in Teflon-sealed glass vessels over appropriate drying agents, and vacuum transferred directly to reaction vessels. Deuterated solvents (Cambridge Isotopes) were dried with appropriate drying agents, vacuum transferred, and stored in an inert atmosphere prior to use. $ZnCl_2$, $Zn(C_6F_5)_2$, and $ZnEt_2$ were purchased from commercial sources in high purity and used without additional purification. $\mathbf{L^{Dipp}}$ was prepared as previously reported,[7e] while $MesN_3$[14] and 4-(diphenylphosphanyl)dibenzofuran[15] were prepared by the standard literature methods. NMR spectra [^{1}H (300.13 MHz), ^{13}C{^{1}H} (75.47 MHz), ^{31}P{^{1}H} (121.48 MHz), ^{19}F (282.42 MHz), and ^{11}B (96.29 MHz)] were collected with a Bruker Avance II NMR spectrometer equipped with a variable-temperature unit. Spectra were collected at ambient temperature and referenced to residual solvent resonances (^{1}H and ^{13}C{^{1}H}), or an external standard [triphenylphosphine (^{31}P{^{1}H}), trifluorotoluene (^{19}F), or boron trifluoride diethyl etherate (^{11}B)]. ^{1}H and ^{13}C NMR peak assignments were facilitated by DEPT, COSY, and HSQC experiments. X-ray crystal data were collected with a Bruker AXS SMART APEX II single-crystal X-ray diffractometer [Mo-K_α (λ = 0.71073 Å)]. Elemental analyses were performed with an Elementar Vario Microcube.

Synthesis of 4-(Mes–N=PPh2)dbf ($\mathbf{L^{Mes}}$): A two-neck 100 mL round–bottom flask attached to a swivel frit apparatus was charged with 4-(diphenylphosphanyl)dibenzofuran (0.67 g, 1.9 mmol). Toluene (approx. 35 mL) was added by vacuum transfer followed by injection of excess $MesN_3$ (0.4634 g, 2.279 mmol). Within minutes of initiating the reaction, evolution of a colorless gas was observed. The reaction mixture was stirred for 12 h at ambient temperature producing a cloudy yellow solution. Filtration to remove residual insoluble impurities yielded a clear yellow solution, which in turn yielded an oily yellow solid upon removal of toluene in vacuo. Pentane (approx. 60 mL) was added by vacuum transfer to the crude product and the mixture was sonicated for approximately 2 min and additionally vigorously stirred for 2 h. Filtration of the resulting suspension afforded $\mathbf{L^{Mes}}$ as a white powder, which was washed three times with 10 mL portions of pentane and dried in vacuo. Total yield was 69 % (0.64 g, 1.3 mmol). **^{1}H NMR** ([D$_6$]benzene): δ = 8.02 (dd, $^2J_{HP}$ = 12.1, $^3J_{HH}$ = 6.0 Hz, 1 H, dbf-C$_3$), 7.91 (dd, $^3J_{HP}$ = 11.3, $^3J_{HH}$ = 5.8 Hz, 4 H, *o*-PPh$_2$), 7.61 (d, $^3J_{HH}$ = 6.9 Hz, 1 H, dbf), 7.49 (m, 1 H, dbf), 7.08–6.93 (br. ov m, 10 H, *m*-PPh$_2$, *p*-PPh$_2$, dbf), 6.88 (s, 2 H, *m*-Mes), 2.30 (s, 6 H, *o*-Mes), 2.21 (s, 3 H, *p*-Mes) ppm. **^{13}C{$_1$H} NMR** ([D$_6$]benzene): δ = 157.1 (d, $^2J_{CP}$ = 3.0 Hz, dbf-quaternary), 156.8 (s, dbf-quaternary), 145.6 (s, dbf-quaternary), 134.7 (d, $^1J_{CP}$ = 105 Hz, dbf-C$_4$), 132.8 (d, $^2J_{CP}$ = 9.1 Hz, *o*-PPh$_2$), 132.7 (s, *p*-Mes *C*CH$_3$), 132.4 (d, $^3J_{CP}$ = 6.0 Hz, *m*-PPh$_2$), 131.5 (d, $^3J_{CP}$ = 3.0 Hz, dbf-C$_2$), 129.7 (s, *o*-Mes ***C***CH$_3$), 129.5 (s, *m*-Mes) 128.8 (d, $^2J_{CP}$ = 12.1 Hz, dbf-C$_3$), 127.7 (s, *ipso*-Mes), 125.4 (s, dbf-quaternary), 124.7 (d, $^4J_{CP}$ = 2.4 Hz, *p*-PPh$_2$), 123.5 (s, dbf), 123.5 (s, dbf), 123.4 (s, dbf), 121.2 (s, dbf), 119.3 (d, $^1J_{CP}$ = 96.6 Hz, *ipso*-PPh$_2$), 112.4 (s, dbf), 22.0 [s, *o*-Mes C(***C***H$_3$)], 21.3 [s, *p*-Mes C(*C*H$_3$)] ppm. **^{31}P{^{1}H} NMR** ([D$_6$]benzene): δ = –15.3 (s) ppm. Anal. for $C_{33}H_{28}NOP$: calcd. C: 81.65; H: 5.81; N: 2.88 %; found: C: 81.16; H: 6.15; N: 2.94 %. X-ray quality single crystals of $\mathbf{L^{Mes}}$ were grown from a saturated solution in toluene at –35 °C.

Synthesis of $\mathbf{L^{Dipp}ZnCl_2}$ (1): $\mathbf{L^{Dipp}}$ (100 mg, 0.190 mmol) and $ZnCl_2$ (25.8 mg, 0.190 mmol) were combined in a bomb with toluene (5 mL), resulting in dissolution of the ligand and a suspension of the zinc dichloride. This mixture was heated to 120 °C for 24 h, resulting in a clear yellow solution with all material dissolved. Allowing the reaction mixture to cool caused the solution to become cloudy. This solution was transferred to a vial and left at ambient temperature to crystallize for 48 h, resulting in the formation of white crystals of the compound. The supernatant was decanted and the crystals were washed with pentane (3 × 1 mL) and dried in vacuo, giving complex **1** in 64.8 % yield (81.5 mg, 0.123 mmol). **^{1}H NMR** (CD_2Cl_2): δ = 8.36 (d, 1 H, $^3J_{HH}$ = 7.7 Hz, 1-dbf), 8.10 (d, 1 H, $^3J_{HH}$ = 7.7 Hz, 9-dbf), 7.91 (br. s, 1 H, 6-dbf), 7.67–7.58 (ov m, 3 H, *p*-Ph + 7-dbf), 7.58–7.37 (ov m, 10 H, *o*-Ph + *m*-Ph + 2-dbf + 8-dbf), 7.18–6.94 (ov m, 4 H, *m*-Dipp + *p*-Dipp + 3-dbf), 3.35 [sp, 2 H, $^3J_{HH}$ = 6.8 Hz, C*H*(CH$_3$)$_2$], 1.21 [d, 6 H, $^3J_{HH}$ = 6.8 Hz, CH(C*H*$_3$)$_2$], 0.23 [d, 6 H, $^3J_{HH}$ = 6.8 Hz, CH(C*H*$_3$)$_2$] ppm. **^{13}C{^{1}H} NMR** (CD_2Cl_2): δ = 158.55 (s, Aromatic C), 156.36 (s, Aromatic C), 147.16 (d, $^3J_{CP}$ = 5.4 Hz, Aromatic C), 138.51 (d, $^3J_{CP}$ = 7.9 Hz, Aromatic C), 134.72 (d, $^2J_{CP}$ = 10.0 Hz, *o*-Ph), 134.18 (d, $^2J_{CP}$ = 11.1 Hz, 3-dbf), 133.90 (d, $^4J_{CP}$ = 2.6 Hz, *p*-Ph), 129.68 (s, 8-dbf), 129.48 (d, $^3J_{CP}$ = 12.5 Hz, *m*-Ph), 127.43 (s, 1-dbf), 127.08 (d, $^1J_{CP}$ = 97.1 Hz, *ipso*-Ph), 126.30 (d, $^5J_{CP}$ = 3.5 Hz, *p*-Dipp), 125.23 (s, 7-dbf), 124.71 (d, $^3J_{CP}$ = 2-dbf), 124.62 (d, $^4J_{CP}$ = 5.0 Hz, *m*-Dipp), 123.00 (s, Aromatic C), 121.63 (s, 9-dbf), 113.53 (s, 6-dbf), 109.74 (d, $^1J_{CP}$ = 112.8 Hz, 4-dbf), 29.39 [s, *C*H(CH$_3$)$_2$], 25.72 (s, CH(*C*H$_3$)$_2$], 22.62 (CH(*C*H$_3$)$_2$] ppm. One quaternary ^{13}C signal was not observed. **^{31}P{^{1}H} NMR** (CD_2Cl_2): δ = 30.46 (s) ppm. Anal. for $C_{36}H_{34}Cl_2NOPZn$: calcd. C: 65.12; H: 5.16; N: 2.11 %; found: C: 64.82; H: 4.94; N: 2.44 %.

Synthesis of $\mathbf{L^{Mes}ZnCl_2}$ (2): $\mathbf{L^{Mes}}$ (200 mg, 0.412 mmol) and $ZnCl_2$ (56.1 mg, 0.412 mmol) were combined in a bomb with toluene (20 mL). The resulting suspension was heated to 120 °C with stirring for a period of 48 h. During this time, $ZnCl_2$ was observed to eventually dissolve, followed by gradual formation of a white precipitate. The volume of toluene was reduced to 10 mL in vacuo, and an equiva-

Zeitschrift für anorganische und allgemeine Chemie ZAAC Journal of Inorganic and General Chemistry

lent amount of pentane was added to encourage complete precipitation of the product. The solvent was decanted and the resulting white solid was dried in a vacuum, giving complex **2** in 88.6% yield (227 mg, 0.365 mmol). **^{1}H NMR** (CD_2Cl_2): δ = 8.19 (d, 1 H, $^3J_{HH}$ = 7.7 Hz, 1-dbf), 7.93 (d, 1 H, $^3J_{HH}$ = 7.7 Hz, 9-dbf), 7.75 (dd, 4 H, $^3J_{PH}$ = 12.7, $^3J_{HH}$ = 7.7 Hz, *o*-Ph), 7.67 (tq, 2 H, $^3J_{HH}$ = 7.7, $^4J_{HH}$ = 1.8, $^5J_{PH}$ = 1.8 Hz, *p*-Ph), 7.51 (td, 4 H, $^3J_{HH}$ = 7.7, $^4J_{PH}$ = 3.5 Hz, *m*-Ph), 7.45 –7.23 (ov m, 5 H, 2-dbf + 3-dbf + 6-dbf + 7-dbf + 8-dbf), 6.45 (s, 2 H, *m*-Mes), 2.01 (s, 6 H, *o*-CH_3Mes), 1.87 (s, 3 H, *p*-CH_3Mes) ppm. **^{31}P{^{1}H} NMR** (CD_2Cl_2): δ = 28.0 (s) ppm. Anal. for $C_{33}H_{28}Cl_2NOPZn$: calcd. C: 63.74; H: 4.54; N: 2.25%; found: C: 64.16; H: 4.75; N: 2.18%.

Synthesis of $L^{Dipp}Zn(C_6F_5)_2$ (3): L^{Dipp} (100 mg, 0.190 mmol) and $Zn(C_6F_5)_2$ (76.0 mg, 0.190 mmol) were combined in a scintillation vial and dissolved in toluene (1 mL), giving a clear yellow solution. This solution was layered with pentane (3 mL) and placed in a –35 °C freezer. White crystals of the compound formed after four days. The supernatant was decanted, the crystals were washed with pentane (3 × 1 mL) and dried in vacuo, giving complex **3** in 81.1% yield (143 mg, 0.154 mmol). **^{1}H NMR** (C_6D_6): δ = 7.59 (d, 1 H, $^3J_{HH}$ = 8.0 Hz, 9-dbf), 7.56–7.48 (ov m, 2 H, 6-dbf + 1-dbf), 7.32 (br. m, 4 H, *o*-Ph), 7.22–7.12 (m, 1 H, obscured by solvent, 8-dbf), 7.12–6.87 (ov m, 6 H, 7-dbf + *p*-Dipp + *m*-Dipp + *p*-Ph), 6.80 (td, 4 H, $^3J_{HH}$ = 7.7, $^3J_{PH}$ = 3.0 Hz, *m*-Ph), 6.76–6.68 (ov m, 2 H, 2-dbf + 3-dbf), 3.84 [sp, 2 H, $^3J_{HH}$ = 6.7 Hz, C*H*(CH_3)$_2$], 1.11 [d, 6 H, $^3J_{HH}$ = 6.7 Hz, CH(CH_3)$_2$] 0.38 [d, 6 H, $^3J_{HH}$ = 6.7 Hz, CH(CH_3)$_2$] ppm. **^{13}C{^{1}H} NMR** (C_6D_6): δ = 158.23 (s, Aromatic C), 156.88 (s, Aromatic C), 148.58 (br. dd, $^1J_{CF}$ = 226, $^2J_{CF}$ = 28 Hz, *o*-C_6F_5), 147.41 (d, J_{CP} = 5.8 Hz, Aromatic C), 140.34 (br. d, $^1J_{CF}$ = 238 Hz, *p*-C_6F_5), 139.74 (d, J_{CP} = 8.2 Hz, Aromatic C), 137.04 (br. d, $^1J_{CF}$ = 248 Hz, *m*-C_6F_5), 134.32 (d, $^2J_{PC}$ = 9.7 Hz, *o*-Ph), 133.88 (d, $^4J_{CP}$ = 2.4 Hz, *p*-Ph), 133.76 (s, 3-dbf), 129.39 (s, 7-dbf), 129.33 (d, $^3J_{CP}$ = 12.4 Hz, *m*-Ph), 126.89 (d, $^4J_{CP}$ = 2.7 Hz, 1-dbf), 126.66 (d, $^5J_{CP}$ = 3.6 Hz, *p*-Dipp), 126.64 (br. d, $^1J_{PC}$ = 101.5 Hz, *ipso*-Ph), 126.30 (d, J_{CP} = 6.8 Hz, Aromatic C), 125.18 (d, $^4J_{CP}$ = 3.4 Hz, *m*-Dipp), 124.61 (s, 8-dbf), 123.68 (d, $^3J_{PC}$ = 11.3 Hz, 2-dbf), 123.31 (br. t, $^2J_{CF}$ = 70 Hz, *ipso*-C_6F_5), 122.69 (d, J_{CP} = 0.9 Hz, Aromatic C), 121.04 (s, 9-dbf), 113.31 (s, 6-dbf), 111.10 (d, $^1J_{PC}$ = 100.6 Hz, 4-dbf), 29.04 [s, *C*H(CH_3)$_2$], 25.28 [s, CH(*C*H_3)$_2$], 23.96 [s, CH(CH_3)$_2$] ppm. **^{19}F{^{1}H} NMR** (C_6D_6): δ = –114.51 (m, 4F, *o*-C_6F_5), –156.83 (t, 2F, *p*-C_6F_5), –160.82 (m, 4F, *m*-C_6F_5) ppm. **^{31}P{^{1}H} NMR** (C_6D_6): δ = 28.5 (s) ppm. Anal. for $C_{48}H_{34}F_{10}NOPZn$: calcd. C: 62.18; H: 3.70; N: 1.51%; found: C: 62.27; H: 3.92; N: 1.95%.

Synthesis of $L^{Mes}Zn(C_6F_5)_2$ (4): Complex **4** was prepared similarly to **3** using L^{Mes} (100 mg, 0.206 mmol) and $Zn(C_6F_5)_2$ (82.3 mg, 0.206 mmol), affording pale yellow crystals of **4** in 87.8% yield (160 mg, 0.181 mmol). **^{1}H NMR** (C_6D_6): δ = 7.60–7.45 (ov m, 3 H, 1-dbf + 6-dbf + 9-dbf), 7.38 (dd, 4 H, $^3J_{PH}$ = 12.5, $^3J_{HH}$ = 7.9 Hz, *o*-Ph), 7.20–7.10 (ov m, 1 H, 7-dbf, obscured by solvent signal), 7.06 (td, 1 H, $^3J_{HH}$ = 7.5, 4*J*HH = 1.1 Hz, 8-dbf), 6.94 (tq, 2 H, $^3J_{HH}$ = 7.7, $^4J_{HH}$ = 1.5, $^5J_{PH}$ = 1.5 Hz, *p*-Ph), 6.86–6.72 (ov m, 6 H, *m*-Ph + 2-dbf + 3-dbf), 6.39 (s, 2 H, *m*-Mes), 2.12 (s, 6 H, *o*-CH_3Mes), 1.84 (s, 3 H, *p*-CH_3Mes) ppm. **^{13}C{^{1}H} NMR** (C_6D_6): δ = 157.67 (s, Aromatic C), 156.29 (s, Aromatic C), 148.03 (br. dd, $^1J_{CF}$ = 222, $^2J_{CF}$ = 28 Hz, *o*-C_6F_5), 140.03 (d, J_{CP} = 7.6 Hz, Aromatic C), 139.60 (br. d, $^1J_{CF}$ = 240 Hz, *p*-C_6F_5), 136.27 (br. d, $^1J_{CF}$ = 250 Hz, *m*-C_6F_5), 136.10 (d, J_{CP} = 5.7 Hz, Aromatic C), 133.80 (d, J_{CP} = 3.9 Hz, Aromatic C), 133.49 (d, $^2J_{CP}$ = 9.9 Hz, *o*-Ph), 133.20 (d, $^4J_{CP}$ = 2.9 Hz, *p*-Ph), 131.95 (d, $^3J_{CP}$ = 8.4 Hz, 3-dbf), 129.40 (d, $^4J_{CP}$ = 3.3 Hz, *m*-Mes), 128.66 (s, 7-dbf), 128.52 (d, $^3J_{CP}$ = 12.5 Hz, *m*-Ph), 126.13 (d, $^4J_{CP}$ = 2.7 Hz, 1-dbf), 126.03 (d, $^1J_{CP}$ = 103.0 Hz, *ipso*-Ph), 125.79 (d, J_{CP} = 6.6 Hz, Aromatic C), 123.86 (s, 8-dbf), 122.89 (d, $^3J_{CP}$ = 11.3 Hz, 2-dbf), 122.11 (t, $^2J_{CF}$ = 67 Hz, *ipso*-C_6F_5), 122.08 (s, Aromatic C), 120.48 (s, 9-dbf), 112.95 (s, 6-dbf), 111.17 (d, $^1J_{CP}$ = 99.0 Hz, 4-dbf), 20.70 (br. s, *o*-*C*H_3Mes), 20.10 (d, $^6J_{CP}$ = 1.4 Hz, *p*-CH_3Mes) ppm. **^{19}F{^{1}H} NMR** (C_6D_6): δ = –114.53 (m, 4F, *o*-C_6F_5), –157.07 (t, 2F, *p*-C_6F_5), –161.27 (m, 4F, *m*-C_6F_5) ppm. **^{31}P{^{1}H} NMR** (C_6D_6): δ = 25.7 (s) ppm. Anal. for $C_{45}H_{28}F_{10}NOPZn{\cdot}C_5H_{12}$: calcd. C: 62.74; H: 4.21; N: 1.46%; found: C: 62.67; H: 3.96; N: 1.43%.

Synthesis of $L^{Dipp}{}_2Zn_3(\mu\text{-}SO_3CF_3)_4(\mu\text{-}OCH_3)_2$ (5): In a 20 mL Teflon-sealed vial, a stoichiometric amount of dry methanol (5.2 µL, 0.13 mmol) was added to a suspension of $L^{Dipp}ZnEt(OTf)$ (100 mg, 0.130 mmol) in benzene (3 mL). The vial was sealed, heated to 100 °C for 1 h, and afterwards cooled to ambient temperature and left to stand for a period of 48 h. A significant amount of material crystallized during that time. The mother liquor was decanted, and the colorless crystals were washed with benzene (2 × 1 mL) and pentane (2 × 1 mL) and dried in vacuo, affording **5** as a white crystalline material in 92.4% yield (57.2 mg, 0.0300 mmol). The compound is essentially insoluble in non-coordinating solvents, thus precluding characterization by NMR spectroscopy. Anal. for $C_{78}H_{74}F_{12}N_2O_{16}P_2S_4Zn_3$: calcd. C: 49.05; H: 3.91; N: 1.47; S: 6.72%; found: C: 49.25; H: 4.07; N: 1.52; S: 6.68%.

X-ray Crystallography: Crystals were grown from hot toluene during the course of the reaction for **1** and **2**, from toluene solutions layered with pentane at –35 °C for L^{Mes}, **3** and **4**, and from benzene solution of the reaction mixture at ambient temperature for **5**. X-ray intensities were measured with a Bruker SMART APEX II instrument (Mo-K_α radiation; λ = 0.71073 Å) at a temperature of 173(2) K. Unit cell parameters were determined and refined on all reflections and data were integrated with APEX2 software.[16] Data reduction and correction for Lorentz polarization were performed using Saint-plus,[17] and scaling and absorption correction were performed using the SADABS software package.[18] Structure solution by direct methods and least-squares refinement on F^2 were performed using the SHELXTL software suite.[19] Non-hydrogen atoms were refined with anisotropic displacement parameters, while hydrogen atoms were placed in calculated positions and refined with a riding model. The SQUEEZE subroutine of the PLATON software package[20] was used to model disordered solvent molecules in **3** and **5** and these solvent molecules are included in the respective formulae. Multi-scan absorption correction was employed in all cases. Structural figures were generated with ORTEP-3.[21] A summary of the crystallographic data and structure refinement results for L^{Mes} and complexes **1**–**5** are listed in Table 4

Crystallographic data (excluding structure factors) for the structures in this paper have been deposited with the Cambridge Crystallographic Data Centre, CCDC, 12 Union Road, Cambridge CB21EZ, UK. Copies of the data can be obtained free of charge on quoting the depository numbers CCDC-833316, -833317, -833318, -833319, -833320, and -833321 (Fax: +44-1223-336-033; E-Mail: deposit@ccdc.cam.ac.uk, http://www.ccdc.cam.ac.uk).

Acknowledgement

P.G.H. thanks *NSERC*, *Canada Foundation for Innovation, Canada School of Energy and Environment* and *GreenCentre Canada* for financial support. *C.A.W.* acknowledges *NSERC*, the *Alberta Ingenuity Fund (Alberta Innovates)* and the *Alberta Heritage Fund* for student awards. *Mr. Tony Montina* of the University of Lethbridge is acknowledged for expert technical assistance.

Table 4. Crystal data and refinement details for L^{Mes} and complexes **1**–**5**.

	L^{Mes}	**1**	**2**	**3**	**4**	**5**
Empirical formula	$C_{33}H_{28}NOP{\cdot}0.5C_7H_8$	$C_{36}H_{34}Cl_2NOPZn$	$C_{66}H_{56}C_{14}N_2O_2P_2Zn_2{\cdot}C_7H_8$	$C_{48}H_{34}F_{10}NOPZn{\cdot}C_7H_8$	$C_{45}H_{28}F_{10}NOPZn{\cdot}C_5H_{12}$	$C_{78}H_{74}F_{12}N_2O_{16}P_2S_4Zn_3$
Formula weight	531.60	663.88	1335.7	1019.24	957.17	1909.68
Temperature / K	173(2)	173(2)	173(2)	173(2)	173(2)	173(2)
Wavelength / Å	0.71073	0.71073	0.71073	0.71073	0.71073	0.71073
Crystal system	triclinic	triclinic	triclinic	triclinic	monoclinic	triclinic
Space group	$P\bar{1}$	$P\bar{1}$	$P\bar{1}$	$P\bar{1}$	$P2_1/n$	$P\bar{1}$
a /Å	9.1830(5)	9.3247(4)	9.5777(5)	12.3644(7)	15.274(1)	12.729(2)
b /Å	14.4232(7)	10.7683(4)	13.5073(7)	13.2795(7)	14.196(1)	13.861(2)
c /Å	11.2504(6)	16.9837(7)	14.889(1)	17.704(1)	21.311(2)	14.226(2)
α /°	86.958(1)	78.32	114.568(1)	70.327(1)	90	86.308(1)
β /°	82.190(1)	83.58	92.957(1)	70.849(1)	98.317(1)	89.135(1)
γ /°	75.102(1)	75.89	108.823(1)	71.903(1)	90	84.456(1)
Volume /Å^3	1426.4(1)	1616.1(1)	1619.1(2)	2519.4(2)	4572.3(7)	2492.9(5)
Z	2	2	2	2	4	2
ρ calcd. / Mg·m^{-3}	1.238	1.364	1.370	1.344	1.390	1.272
μ /mm^{-1}	0.126	1.004	1.003	0.595	0.651	0.908
F(000)	562	688	690	1044	1960	976
Crystal size / mm	0.46 × 0.24 × 0.12	0.39 × 0.32 × 0.25	0.24 × 0.17 × 0.12	0.30 × 0.26 × 0.24	0.30 × 0.26 × 0.18	0.28 × 0.26 × 0.13
θ range /°	2.31 to 25.03	2.64 to 26.37	2.60 to 26.37	2.56 to 25.03	2.62 to 25.03°.	2.59 to 25.03
Reflections collected	13790	17389	21637	24263	43393	23701
Independent reflections	5017 [R(int) = 0.0156]	6576 [R(int) = 0.0115]	6586 [R(int) = 0.0283]	8863 [R(int) = 0.0219]	8076 [R(int) = 0.0310]	8770 [R(int) = 0.0381]
Completeness to θ = 25.03°	99.6 %	99.2 %	99.5 %	99.6 %	99.9 %	99.6 %
Data / restraints / parameters	5017 / 4 / 380	6576 / 0 / 383	6586 / 99 / 407	8863 / 0 / 615	8076 / 0 / 582	8770 / 0 / 534
Goodness-of-fit (GOF)	1.028	1.068	1.034	1.045	1.025	1.023
R indices [$I > 2\sigma(I)$]	R_1 = 0.0333, wR_2 = 0.0845	R_1 = 0.0223, wR_2 = 0.0612	R_1 = 0.0377, wR_2 = 0.0979	R_1 = 0.0366, wR_2 = 0.0998	R_1 = 0.0365, wR_2 = 0.0883	R_1 = 0.0408, wR_2 = 0.1026
R indices (all data)	R_1 = 0.0378, wR_2 = 0.0876	R_1 = 0.0238, wR_2 = 0.0620	R_1 = 0.0495, wR_2 = 0.1051	R_1 = 0.0433, wR_2 = 0.1033	R_1 = 0.0513, wR_2 = 0.0972	R_1 = 0.0664, wR_2 = 0.1102
Largest diff. peak/hole / e·Å^{-3}	0.291 and –0.350	0.394 and –0.251	1.531 and –0.359	0.553 and –0.479	0.482 and –0.304	0.645 and –0.329

References

[1] For recent reviews see: a) T. K. Panda, P. W. Roesky, *Chem. Soc. Rev.* **2009**, *38*, 2782–2804; b) T. Cantat, N. Mezailles, A. Auffrant, P. Le Floch, *Dalton Trans.* **2008**, 1957–1972; c) A. Steiner, S. Zacchini, P. I. Richards, *Coord. Chem. Rev.* **2002**, *227*, 193–216.

[2] See for example: a) A. Ramos, D. W. Stephan, *Dalton Trans.* **2010**, *39*, 1328–1338; b) O. Alhomaidan, C. Beddie, G. C. Bai, D. W. Stephan, *Dalton Trans.* **2009**, 1991–1998; c) K. D. Conroy, W. E. Piers, M. Parvez, *J. Organomet. Chem.* **2008**, *693*, 834–846; d) M. J. Sarsfield, M. Said, M. Thornton-Pett, L. A. Gerrard, M. Bochmann, *J. Chem. Soc. Dalton Trans.* **2001**, 822–827; e) R. P. K. Babu, R. McDonald, R. G. Cavell, *Chem. Commun.* **2000**, 481–482.

[3] See for example: a) C. C. Brown, C. Glotzbach, D. W. Stephan, *Dalton Trans.* **2010**, *39*, 9626–9632; b) K. Chan, L. Spencer, J. Masuda, J. McCahill, P. Wei, D. W. Stephan, *Organometallics* **2004**, *23*, 381–390; c) S. Al-Benna, M. J. Sarsfield, M. Thornton-Pett, D. L. Ormsby, P. J. Maddox, P. Bres, M. Bochmann, *J. Chem. Soc. Dalton Trans.* **2000**, 4247–4257; d) J. Li, A. A. Pinkerton, D. C. Finnen, M. Kummer, A. Martin, F. Wiesemann, R. G. Cavell, *Inorg. Chem.* **1996**, *35*, 5684–5692.

[4] See for example: a) J. Jenter, P. W. Roesky, N. Ajellal, S. M. Guillaume, N. Susperregui, L. Maron, *Chem. Eur. J.* **2010**, *16*, 4629–4638; b) A. Buchard, R. H. Platel, A. Auffrant, X. F. Le Goff, P. Le Floch, C. K. Williams, *Organometallics* **2010**, *29*, 2892–2900; c) K. R. D. Johnson, P. G. Hayes, *Organometallics* **2009**, *28*, 6352–6361; d) M. Rastatter, A. Zulys, P. W. Roesky, *Chem. Eur. J.* **2007**, *13*, 3606–3616.

[5] See for example: a) S. Courtenay, D. Walsh, S. Hawkeswood, P. R. Wei, A. K. Das, D. W. Stephan, *Inorg. Chem.* **2007**, *46*, 3623–3631; b) G. C. Welch, W. E. Piers, M. Parvez, R. McDonald, *Organometallics* **2004**, *23*, 1811–1818; c) P. R. Wei, D. W. Stephan, *Organometallics* **2003**, *22*, 601–604.

[6] See for example: a) C. V. Cárdenas, M. A. M. Hernández, J.-M. Grévy, *Dalton Trans.* **2010**, *39*, 6441–6448; b) C. J. Wallis, I. L. Kraft, B. O. Patrick, P. Mehrkhodavandi, *Dalton Trans.* **2010**, *39*, 541–547; c) S. Marks, T. K. Panda, P. W. Roesky, *Dalton Trans.* **2010**, *39*, 7230–7235; d) A. Murso, D. Stalke, *Eur. J. Inorg. Chem.* **2004**, 4272–4277; e) M. S. Hill, P. B. Hitchcock, *J. Chem. Soc. Dalton Trans.* **2002**, 4694–4702; f) S. Wingerter, H. Gornitzka, G. Bertrand, D. Stalke, *Eur. J. Inorg. Chem.* **1999**, 173–178.

[7] a) C. A. Wheaton, P. G. Hayes, *Organometallics* submitted; b) B. J. Ireland, C. A. Wheaton, P. G. Hayes, *Organometallics* **2010**, *29*, 1079–1084; c) C. A. Wheaton, P. G. Hayes, *Dalton Trans.* **2010**, *39*, 3861–3869; d) C. A. Wheaton, P. G. Hayes, *Chem. Commun.* **2010**, *46*, 8404–8406; e) C. A. Wheaton, B. J. Ireland, P. G. Hayes, *Organometallics* **2009**, *28*, 1282–1285.

[8] a) A. Charafeddine, W. Dayoub, H. Chapuis, P. Strazewski, *Chem. Eur. J.* **2007**, *13*, 5566–5584; b) S. Bräse, C. Gil, K. Knepper, V. Zimmermann, *Angew. Chem. Int. Ed.* **2005**, *44*, 5188–5240.

[9] a) C. J. Wallis, I. L. Kraft, J. N. Murphy, B. O. Patrick, P. Mehrkhodavandi, *Organometallics* **2009**, *28*, 3889–3895; b) K. T. K. Chan, L. P. Spencer, J. D. Masuda, J. S. J. McCahill, P. Wei, D. W. Stephan, *Organometallics* **2004**, *23*, 381–390.

[10] M. D. Hannant, M. Schormann, M. Bochmann, *J. Chem. Soc. Dalton Trans.* **2002**, 4071–4073.

[11] For recent reviews discussing lactide polymerization see: a) M. J.

Stanford, A. P. Dove, *Chem. Soc. Rev.* **2010**, *39*, 486–494; b) C. A. Wheaton, P. G. Hayes, B. J. Ireland, *Dalton Trans.* **2009**, 4832–4846; c) R. H. Platel, L. M. Hodgson, C. K. Williams, *Polym. Rev.* **2008**, *48*, 11–63; d) J. C. Wu, T. L. Yu, C. T. Chen, C.-C. Lin, *Coord. Chem. Rev.* **2006**, *250*, 602–626.

[12] W. Clegg, I. R. Little, B. P. Straughan, *J. Chem. Soc. Chem. Commun.* **1985**, 73–74.

[13] For select recent examples see: a) X. X. Zhou, H. C. Fang, Y. Y. Ge, Z. Y. Zhou, Z. G. Gu, X. Gong, G. Zhao, Q. G. Zhan, R. H. Zeng, Y. P. Cai, *Cryst. Growth Des.* **2010**, *10*, 4014–4022; b) I. Garcia-Santos, J. Sanmartin, A. M. Garcia-Deibe, M. Fondo, E. Gomez, *Polyhedron* **2009**, *28*, 3055–3059; c) K. F. Konidaris, M. Kaplanis, C. P. Raptopoulou, S. P. Perlepes, E. Manessi-Zoupa, E. Katsoulakou, *Polyhedron* **2009**, *28*, 3243–3250.

[14] T. Tsuritani, H. Mizuno, N. Nonoyama, S. Kii, A. Akao, K. Sato, N. Yasuda, T. Mase, *Org. Process Res. Dev.* **2009**, *13*, 1407–1412.

[15] M. Haenel, D. Jakubik, E. Rothenberger, G. Schroth, *Chem. Ber.* **1991**, *124*, 1705–1710.

[16] *APEX2*, Version 2.1–4; Data Collection and Refinement Program. Bruker AXS, Madison, WI, **2006**.

[17] *SAINT-Plus*, Version 7.23a; Data Reduction and Correction Program. Bruker AXS, Madison, WI, **2004**.

[18] G. M. Sheldrick, *SADABS*, Area-Detector Absorption Correction, v2.10, Universität Göttingen, Germany **1999**.

[19] G. M. Sheldrick, *Acta Crystallogr. Sect. A* **2008**, *64*, 112–122.

[20] A. L. Spek, *Acta Crystallogr. Sect. D* **2009**, *65*, 148–155.

[21] *ORTEP-III*, Oak Ridge Thermal Ellipsoid Plot Program for Crystal Structure Illustrations, M. N. Burnett, C. K. Johnson, Oak Ridge National Laboratory Report ORNL-6895, **1996**.

Received: August 03, 2011
Published Online: September 13, 2011

